Heliyon 10 (2024) e33862

Contents lists available at ScienceDirect

Heliyon

journal homepage: www.cell.com/heliyon

Research article

Modelling and optimization of fenton process for decolorization of azo dye (DR16) at microreactor using artificial neural network and genetic algorithm

Jafar Sadeghzadeh Ahari [a,**], Masoud Sadeghi [a], Mahdi Koolivand Salooki [a], Morteza Esfandyari [b,*], Masoud Rahimi [c], Sanaz Anahid [a]

[a] Gas Research Division - Research Institute of Petroleum Industry (RIPI), P.O. Box: 14665, 137, Tehran, Iran
[b] Department of Chemical Engineering, Faculty of Engineering, University of Bojnord, Bojnord, Iran
[c] Department of Chemical Engineering, CFD Research Center, Razi University, Tagh Bostan, Kermanshah, Iran

ARTICLE INFO

Keywords:
Artificial neural network
Azo dye
Decolorizing
Direct red 16
Fenton process
Genetic algorithm

ABSTRACT

The Fenton process is widely employed for decolorizing industrial wastewater. Therefore, it is imperative to construct a model for optimizing the operational parameters and estimating the efficiency of decolorization within this process. In this study, an artificial neural network (ANN) model was created based on experimental data provided by a previous researcher who examined the decolorization of Direct Red 16 dye (DR16) using a heterogeneous Fenton process within a microchannel reactor. This model was utilized to optimize and forecast the efficiency of decolorization in the Fenton process. The accuracy of the model was validated by comparing its outcomes with actual experimental data. To further improve the efficiency of decolorization, optimal operational parameters were ascertained utilizing the genetic algorithm method. The study revealed that as dye concentrations increased from 10 to 40 mg/l, decolorization efficiencies improved proportionately, peaking at 89.78 %. Optimal operational parameters for maximizing efficiency were identified as a feed flow rate of 1 ml/min, H_2O_2 concentration at 500 mg/l, Fe2+ concentration of 4 mg/l, and maintaining pH between 2.6 and 2.8. Insights derived from both experimental and model-generated data were used to analyze the impact of operational parameters on decolorization efficiency.

Nomenclature

Acronym	Parameter
ANN	Artificial neural network
DR16	Direct Red 16 dye
ARIMA	Autoregressive integrated moving average
MLR	Multiple linear regression
R^2	correlation coefficient
MSE	mean square error
AARE	mean absolute relative error

(*continued on next page*)

* Corresponding author.
** Corresponding author.
E-mail addresses: sadeghzadehj@ripi.ir (J. Sadeghzadeh Ahari), M.Esfandyari@ub.ac.ir (M. Esfandyari), m.rahimi@razi.ac.ir (M. Rahimi).

https://doi.org/10.1016/j.heliyon.2024.e33862
Received 17 February 2024; Received in revised form 10 June 2024; Accepted 27 June 2024
Available online 28 June 2024

(*continued*)

X_{min}	minimum values of the raw data
X_{max}	maximum values of the raw data
n	number of data points
$\overline{X}$	the mean of X over the n samples
Xobs	actual values
Xcal	predicted values

1. Introduction

The textile industry stands out as one of the most significant contributors to pollution due to the substantial quantities of dyes and chemicals it encompasses. The presence of these substances in water significantly contributes to environmental pollution and disrupts the ecosystems of various living organisms [1–3]. With over 100,000 commercial colors available, approximately 7×10^7 tons of dyestuff are produced annually [4–6]. Dye wastewater primarily originates from industries such as papermaking, food processing, cosmetics, sanitation, textiles, dyeing, printing, and tanning [7,8]. Within the realm of aromatic organic dyes, azo dyes represent the most extensive group commonly utilized across diverse industries [9,10].

Due to their ease and cost-effectiveness of synthesis, stability, and wide range of available colors, synthetic dyes have become the primary choice over natural dyes in the textile industry. These dyes typically contain a chromophore group with one or more azo (-N]N-) groups, often conjugated with benzene and/or naphthalene systems. However, the release of these dyes into water bodies poses significant environmental risks, causing aesthetic issues, reducing light penetration, and presenting health hazards such as toxicity, mutagenicity, and carcinogenicity to living organisms [1,11].

It is crucial to effectively treat wastewater contaminated with dyes that are discharged from textile industries in order to prevent the pollution of surface water, soil, and the surrounding environment [2]. In recent times, a range of physicochemical and biological treatment methods have been recommended for the removal of dyes from these industrial wastewater streams [12,13]. Physical techniques like absorption and adsorption involving adsorbents primarily focus on capturing the colored pollutants through the process of adsorption and phase change without altering the fundamental nature of the pollutants [14,15].

Conversely, while chemical treatment methods like oxidation, flocculation, and precipitation offer high treatment effectiveness for color removal, they are met with hesitation due to issues such as high expenses, increased sludge generation, limited applicability across all dye types, and the generation of hazardous carcinogenic byproducts [16,17]. Biotechnological strategies, such as biological treatment methods, have gained global acceptance for treating dye-contaminated wastewater, primarily due to their reduced sludge production, cost efficiency, and environmental friendliness [18,19]. In biological treatment processes, microorganisms play a crucial role in breaking down and treating azo dyes present in wastewater [19,20].

A wide array of dyes are accessible in the market, with 80 % of them being Azo chromophores. Azo dyes are chemical substances that feature Azo groups (-N]N-) bonded to benzene or naphthalene rings within their molecular structure. Numerous techniques have been devised for handling dye pollutants found in the wastewater of textile industries [21,22]. These methods encompass coagulation, ozonation, activated carbon adsorption, flocculation, and Fenton oxidation as effective strategies for dye removal [22,23].

Recent research endeavors have directed their attention towards utilizing the Fenton process as a means to eliminate various types of Azo dyes [22,24]. The Fenton process stands out as a highly efficient and rapid wastewater treatment method, functioning by producing highly reactive hydroxyl radicals from the Fe^{2+} and H_2O_2 reagents [25,26]. An essential benefit of the Fenton process lies in its straightforward nature and the absence of a requirement for intricate equipment. Furthermore, the chemicals employed in this process are readily accessible at affordable prices.

Azo dyes are extensively utilized in various industries such as textiles, paper, leather tanning, printing, coatings, and cosmetics, owing to their rapid chemical stability, diverse color range, vividness, cost-effective production, and other beneficial properties [2,22,27]. However, a portion of these dyes is lost during the manufacturing process, leading to the presence of azo dyes and other hazardous chemicals in the wastewater generated by these industries. Azo dyes consist of chemical compounds with azo groups (-N]N-) attached to benzene or naphtha rings within their molecular framework. Unfortunately, due to their intricate molecular composition, these colors are not easily biodegradable.

The discharge of azo dyes into wastewater adversely impacts the photosynthesis process of aquatic ecosystems by obstructing sunlight penetration and diminishing dissolved oxygen levels. To address pollutants in industrial wastewater, a plethora of methods are available, with the Fenton process emerging as one of the most efficient solutions. The primary advantage of the Fenton process lies in its capability to completely break down pollutants into carbon dioxide, water, and mineral salts using cost-effective and easily attainable chemical substances. Through the combination of hydrogen peroxide and Fe^{2+}, the Fenton process generates OH radicals as potent oxidation agents, facilitating the oxidation and elimination of organic pollutants from the wastewater [22,25,26].

Fenton reactions can be explained as equations (1)–(6):

$$H_2O_2 + Fe^{2+} \rightarrow Fe^{3+} + {}^{\cdot}OH + OH^- \quad (1)$$

$$Fe^{2+} + {}^{\cdot}OH \rightarrow Fe^{3+} + OH^- \quad (2)$$

$$H_2O_2 + {}^{\cdot}OH \rightarrow H_2O + HO_2 \quad (3)$$

$$Fe^{3+} + H_2O_2 \rightarrow Fe^{2+} + H^+ + HO_2^{\cdot} \quad (4)$$

$$^{\cdot}OH + {}^{\cdot}OH \rightarrow H_2O_2 \quad (5)$$

$$^{\cdot}OH + Organic\ Components \rightarrow Products\ (CO_2 + H_2O + Salts) \quad (6)$$

A review of the literature on the Fenton process indicates that the majority of studies have focused on collecting experimental data in batch reactors for decolorization of various types of azo dyes [20,28,29]. Conversely, there is a scarcity of studies exploring the utilization of continuous flow reactors in the Fenton process [16,19,30,31]. In a notable study, Rahimi et al. [22] employed a Y-shaped continuous microchannel reactor to decolorize an Azo dye (DR16) using the Fenton process. Their findings suggest that utilizing microreactors for continuous flow Fenton processes yields higher decolorization efficiency when compared to the conventional use of batch reactors.

Determining operational conditions that enhance the decolorization efficiency of the Fenton process is crucial. In light of the findings presented by Rahimi et al. [22] and the benefits associated with employing microreactors for the decolorization process, our study is dedicated to developing a suitable model for this purpose. Presently, numerous conventional methods exist for predicting water quality, including multiple linear regression (MLR) [18,32], autoregressive integrated moving average (ARIMA) [33,34], among others.

The MLR method's inherent linearity poses a limitation in detecting non-linear relationships among water quality parameters. On the other hand, the ARIMA method's primary drawback lies in its reliance on a linear model assumption [35]. With the continuous enhancement of computing capabilities in modern computers, artificial neural network (ANN) models and data-driven approaches have seen significant advancements. ANN models prove valuable in situations where establishing a mathematical model between input and output data proves challenging. Moreover, artificial neural networks necessitate fewer initial assumptions [18,21,36] and can deliver superior accuracy [37,38] compared to traditional modeling techniques. The capability of artificial neural networks to address non-linear challenges has garnered increased attention in water quality research [39].

Following the establishment of the optimal model, the study delved into examining the impact of operational conditions on decolorization efficiency. Subsequently, the modeling proficiency and the application of the genetic algorithm (GA) optimization method were implemented to derive the optimal values of operating parameters that maximize decolorization efficiency. Given the demonstrated advantage of heightened decolorization efficiency through the utilization of microreactors in the continuous flow Fenton process as opposed to conventional batch reactors, it becomes imperative to identify the operational conditions that would optimize the decolorization efficiency of this process [23,40].

Furthermore, given the distinct advantages of the ANN method in comparison to other approaches, the novelty of this study lies in the creation of an optimal ANN model for modeling the microreactor involved in the Fenton process, as informed by the findings presented by Rahimi et al. [22]. Additionally, following the development of the ANN model, the genetic algorithm (GA) was applied to determine the optimal values of operating parameters aimed at maximizing the decolorization efficiency of the process.

2. Experimental data

For the experiments, a total of 105 samples were meticulously prepared and tested. The prescribed quantity of $FeSO_4{\cdot}7H_2O$ was introduced into the dye solution, followed by pH adjustment of the solution. Flow rates for both feeds were accurately gauged using two distinct flow meters. Subsequently, samples were extracted from the output stream of the microreactor. Analysis of the samples was conducted using a UV spectrophotometer from UNIC Company. The absorption spectrum of the DR16 solution was scrutinized to pinpoint the wavelength of maximum absorption. Next, the decolorization efficiency was determined by assessing the absorption intensity of the solution at 524 nm. In this study, the experimental data documented by Rahimi et al. [22] was harnessed for model development. Their research entailed an exploration of decolorization efficiency under varying experimental conditions, including solution pH, feed flow rate, $FeSO_4$, H_2O_2, and dye concentrations. The range of parameters investigated is detailed in Table 1, with all experiments conducted at a consistent temperature of 25 °C.

Further insights into the experimental setup and procedure can be found in their publication [22]. In a summary, the chemicals utilized in their study, including hydrogen peroxide (H_2O_2, 35 %), ferrous sulfate heptahydrate ($FeSO_4{\cdot}7H_2O$, 99 %), sulfuric acid (H_2SO_4, 98 %), and sodium hydroxide (NaOH), were procured from Merck. The azo dye Direct Red 16 (DR16) with a purity of 99 % was obtained from Alvan Sabet Company in Iran. The decolorization of the DR16 dye was conducted continuously within a microreactor featuring a quartz cover plate. Within this reactor, a Y-shaped Plexiglas microchannel with dimensions of 0.9 mm depth, 1 mm

Table 1
Experimental data ranges used in this study.

Parameter	Range
pH	2–5.5
$[Fe^{2+}]$ (mg/l)	0.5–4
$[H_2O_2]$ (mg/l)	150–500
[DR16] (mg/l)	10–40
Flow rate (ml/min)	1–8
Temperature (°C)	25

width, and 70 mm length was employed. The initial pH of the solutions was adjusted using sulfuric acid and sodium hydroxide, verified using a pH meter. The concentration of the DR16 solution was measured and recorded pre and post each experimentation using a UV–visible spectrophotometer sourced from UNIC Company.

3. Method

3.1. Artificial neural network

Modeling serves as a valuable tool for predicting process outcomes and identifying optimal operating conditions efficiently and cost-effectively. In traditional chemical reactor modeling, the standard approach involves solving mass, energy, and momentum balance equations simultaneously using conventional mathematical techniques. However, in the case of the Fenton Process for decolorizing DR 16 dye, where reaction rates are not readily available, the conventional modeling methods are not applicable. Hence, resorting to black box methods becomes necessary for modeling this process. In this study, the neural network modeling method was employed for this purpose. The utilization of Artificial Neural Networks (ANN) for process modeling has been extensively explored in various scientific and engineering domains, as documented in numerous articles [23,34,41–47]. Artificial neural networks function as dynamic, non-linear systems comprising a multitude of processing units (neurons) interconnected akin to a biological neural network.

Artificial neural networks consist of two main types: feedforward neural networks and recurrent neural networks. In a feedforward neural network, input information flows solely in a forward direction, moving from the input nodes to the output nodes. Each node within a layer is connected to nodes in both the subsequent and preceding layers, creating a unidirectional flow without backward connections. The most prevalent form of a feedforward neural network is the Multilayer Perceptron (MLP), which typically comprises an input layer, an output layer, and one or more hidden layers. The number of nodes in the input and output layers corresponds to the number of input variables and the number of variables to be predicted, respectively. Determining the optimal structure of the hidden layers, their nodes, and the transfer functions between layers often involves an iterative process of trial and error. This iterative approach allows for the exploration of various network architectures, ultimately aiming to identify a structure with fewer layers and nodes that minimizes prediction errors [4,18,21].

In this investigation, a combination of statistical and graphical criteria was employed to identify the most suitable network architecture. The statistical metrics utilized for evaluation included the correlation coefficient (R^2), mean square error (MSE), and mean absolute relative error (AARE). In an ideal scenario, the optimal values for R^2 is 1.0, and for both MSE and AARE, it is 0.0. These statistical indicators are determined as described in equations (7)–(9):

$$R^2 = 1 - \frac{\sum_{i=1}^{n} (X_{obs} - X_{cal})^2}{\sum_{i=1}^{n} (X_{obs} - \overline{X}_{cal})^2} \tag{7}$$

$$MSE = \frac{1}{n} \sum_{h=1}^{n} (X_{obs} - X_{cal})^2 \tag{8}$$

$$AARE = \frac{1}{n} \sum \left| \frac{X_{obs} - X_{cal}}{X_{obs}} \right| * 100 \tag{9}$$

Where 'n' represents the number of data points, and $\overline{X}$ is the mean of X across the n samples, with X_{obs} and X_{cal} denoting the actual and predicted values, respectively. Meanwhile, the graphical criterion assesses the model's quality based on the proximity of all data point pairs to the $X_{obs} = X_{cal}$ line (referred to as the first bisectrix).

3.2. Genetic algorithm

John Holland introduced the genetic optimization method in 1975 at Michigan State University, drawing inspiration from Darwin's theory of evolution. This approach stands out from traditional optimization techniques as it operates as a parallel and evolutionary search method that does not rely on calculating derivatives of the objective function to identify optimal solutions. A notable advantage of this method over classical approaches is its resistance to the initial starting point's influence on optimization outcomes. Consequently, the likelihood of encountering a local optimum is significantly minimized when utilizing this method [48].

4. Result and discussion

4.1. Experimental

The experimental study of this research reports on the decolorization of an Azo dye (DR16) in a Y-shaped microreactor utilizing the Fenton process. The impact of key operational parameters—such as dye, H_2O_2, and Fe^{2+} concentrations, solution pH, and feed flow rates—on decolorization efficiency under continuous conditions is explored. The findings demonstrated that within pH levels ranging from 3 to 4, higher disappearance of DR16 was observed in the feed stream. Additionally, greater decolorization efficiencies were

achieved with elevated Fe^{2+} and H_2O_2 concentrations, lower dye concentration, and reduced feed flow rate. Remarkably, an efficiency of 86 % for DR16 dye decolorization was attainable in just 4.2 s of residence time using this microreactor, attributed to effective mixing of reactants at the microreactor's mixing point. This research underscores the advantages of employing microreactors for continuous flow decolorization processes compared to traditional batch stirred tank reactors. Further investigations performed by other scientists elaborated the technical aspect of this research summarized bellow briefly.

In 2021, Cruz and colleagues undertook a study on the degradation of Acid Black 210 dye in synthetic and industrial effluents, leveraging a $CoFe_2O_4$/NOM magnetic hybrid catalyst. Their research demonstrated that the heterogeneous electro-Fenton process outperformed the generation of hydrogen peroxide in terms of efficiency. Remarkably, the catalyst, crafted using an environmentally friendly solvent, sustained exceptional activity over multiple uses, leading to significant advancements in contaminant removal [4].

In 2022, Kumar and Gupta delved into the electrochemical oxidation of Direct Blue 86 dye using a Ti electrode coated with a mixed-metal oxide. Their research elucidated the ideal parameters for maximizing dye and COD removal, leading to complete dye mineralization. Moreover, the study delved into degradation pathways, modeling techniques, and projected treatment expenses, underscoring the method's efficacy in treating textile wastewater [49].

In 2022, Bravo-Yumi and colleagues directed their efforts toward the electrochemical oxidation of diverse azo dyes, including mono-azo, diazo, and tetra-azo variants often encountered in the tannery sector. By pinpointing the optimal conditions for effective oxidation, their work resulted in substantial color removal and COD degradation while maintaining low energy usage. Furthermore, the investigation delved into the transformation of carboxylic acids to gauge the extent of dye oxidation [36].

In 2023, Chi and collaborators delved into the remediation of Reactive Red 2 azo dye wastewater via the Electro-Ce(III) (E-Ce(III)) process. Through meticulous exploration of the optimal operational parameters to attain heightened removal efficiencies, the study unraveled the underlying mechanisms and energy utilization of the process. The E-Ce(III) approach demonstrated significant potential in fostering efficient dye degradation, characterized by minimal energy consumption and improved biodegradability of wastewater. These findings underscore its viability as a sustainable water treatment technique [7].

4.2. Predictive modeling with artificial neural network

To ascertain the dye concentration in the output stream, several ANN architectures were devised. These networks were constructed utilizing the Neural Network Toolbox within MATLAB (R2020b) software. Given its efficient convergence capability, the Back-propagation training method employing the Levenberg-Marquardt algorithm was selected. To expedite convergence and enhance the neural network's accuracy, all data were normalized within the range of −1 to 1 using the following equation (10).

$$X_n = \frac{2(X - X_{min})}{X_{max} - X_{min}} - 1 \tag{10}$$

where X_{min} and X_{max} are the minimum and maximum values of the raw data.

Following the normalization of the experimental data comprising 105 data points, they were randomly partitioned into two distinct sets. The training data set, constituting 70 % of the total data, was employed to estimate neural network parameters (weights and biases), while the remaining 30 % formed the test data set for network validation. In Table 2, the statistical outcomes and specifics of the chosen neural network model, determined by the lowest error metrics (MSE and AARE) and the highest R^2 value, are elaborated upon.

As indicated in Table 2, the ideal neural network configuration for predicting the effluent color concentration comprises an input layer, a hidden layer, and an output layer. The respective neuron counts in these layers are 5, 5, and 1, illustrated in Fig. 1.

The activation function in developed model and for the hidden layer and the output layer is tansig (Eq. (11)).

$$f(x) = \frac{1 - e^{-x}}{1 + e^{-x}} \tag{11}$$

The input parameters for this neural network encompass the inlet flow rate, pH level, and the concentrations of Fe^{2+}, H_2O_2, and dye. The network's output corresponds to the dye concentration in the outlet flow. Graphical representations are detailed in Fig. 2, depicting the assessment of the final neural network model's efficacy in predicting decolorization efficiency. Notably, the parity plot illustrates the close clustering of all points around the first bisectrix, emphasizing the model's accuracy. Overall, the statistical and graphical evaluations affirm the proposed model's strong alignment with experimental findings.

Table 2
Statistic results and details of the final neural network model.

No. of Hidden Layer	1
No. of Nodes	5-5-1
Type of Transfer Function	tangsig-tansig
R^2(Train)	0.997
MSE(Train)	5.05e-4
AARE%(Train)	2.28
R^2(Test)	0.995
MSE(Test)	6.34e-4
AARE%(Test)	2.38

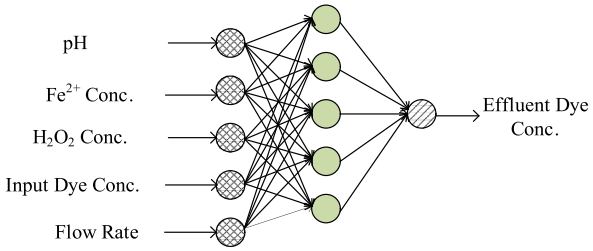

Fig. 1. A three-layer feed-forward neural network used for prediction of effluent Dye concentration.

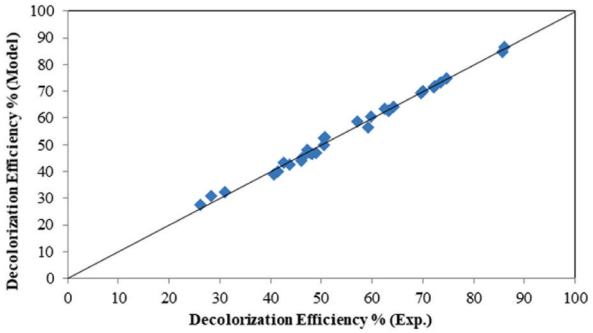

Fig. 2. Comparison between the actual test data set and the ANN model predictions for Decolorization efficiency%.

4.3. *Effect of operating parameters*

The effectiveness of the developed ANN model in simulating the Fenton process was evaluated through a comparison of predicted and experimental data on decolorization efficiency. Simulations involved adjusting two key operating parameters while holding the remaining parameters constant (refer to Figs. 3–6). The outcomes validate that the ANN model, which was created, can reliably forecast the decolorization efficiency of the Fenton process with a high degree of accuracy.

The efficiency of oxidizing organic pollutants, such as azo dyes, through the Fenton process is directly linked to the concentration of oxidants introduced into the reaction medium (solution). Hydrogen peroxide (H_2O_2) serves as the primary oxidant in the Fenton process. The impact of varying H_2O_2 concentrations on decolorization efficiency is depicted in Fig. 3, showcasing the influence at H_2O_2 concentrations of 150 mg/l, 250 mg/l, and 500 mg/l while maintaining a consistent DR16 concentration, ferrous ion concentration, solution pH, and temperature at 30 mg/l, 1 mg/l, 3.5, and 25 °C, respectively. The data demonstrates a positive correlation between higher H_2O_2 concentrations within the range of 150 mg/l to 500 mg/l, at a constant feed flow rate, and enhanced decolorization efficiency. This trend is attributed to the rise in hydroxyl ion concentration with increasing H_2O_2 levels, consequently elevating the degradation reaction rate (as per Eq. (6)) and overall process performance.

The impact of pH on decolorization efficiency was explored across various feed flow rates. As illustrated in Fig. 4, at a consistent

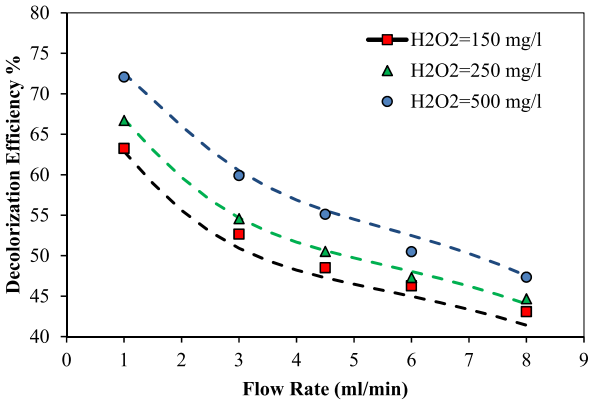

Fig. 3. Comparison between the actual data (symbols) and the ANN model predictions (dashed lines) for Decolorization efficiency% as a function of feed flow rate at several H_2O_2 concentrations (DR16 = 30 mg/l, pH = 3.5, Fe^{2+} = 1 mg/l, T = 25 °C).

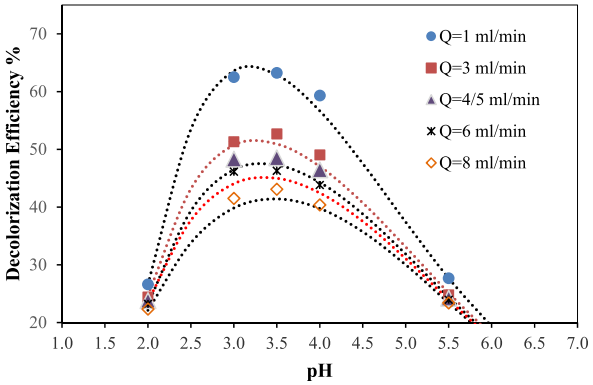

Fig. 4. Comparison between the actual data (symbols) and the ANN model predictions (dashed lines) for Decolorization efficiency% as a function of pH at several feed flow rates (DR16 = 30 mg/l, H_2O_2 = 150 mg/l, Fe^{2+} = 1 mg/l, T = 25 °C).

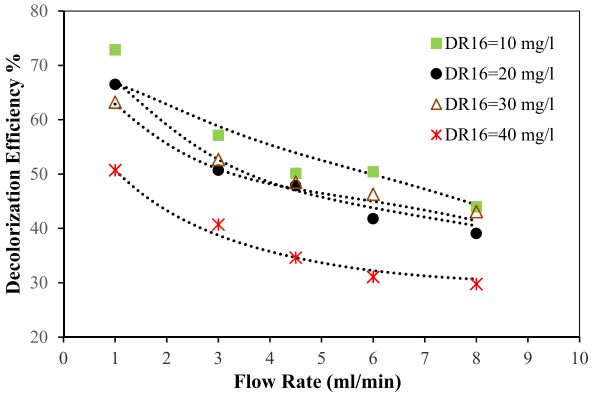

Fig. 5. Comparison between the actual data (symbols) and the ANN model predictions (dashed lines) for Decolorization efficiency% as a function of feed flow rate at several dye concentrations (pH = 3.5, H_2O_2 = 150 mg/l, Fe^{2+} = 1 mg/l, T = 25 °C).

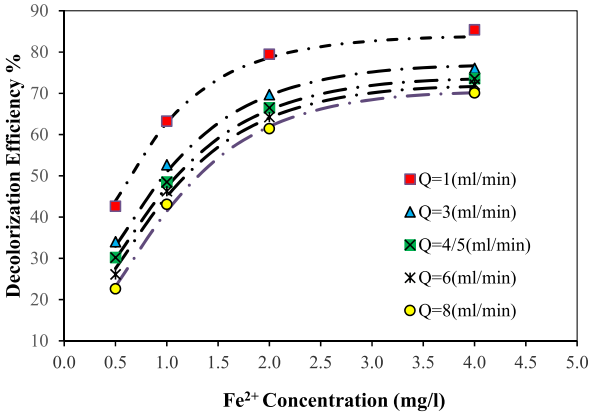

Fig. 6. Comparison between the actual data (symbols) and the ANN model predictions (dashed lines) for Decolorization efficiency% as a function of Fe^{2+} concentration at several feed flow rates (pH = 3.5, H_2O_2 = 150 mg/l, DR16 = 30 mg/l, T = 25 °C).

feed flow rate, increasing the pH initially enhances decolorization efficiency up to a peak level before exhibiting a decline. The pH level plays a critical role in the generation of free radicals and consequently influences the effectiveness of the Fenton process. It is widely acknowledged that at pH levels below the optimal range (around 2.5–3.5), hydrogen peroxide (H_2O_2) reacts with excess H+ ions to form oxonium ions ($H_3O_2^+$), which are stable and do not engage in the production of hydroxyl radicals. This circumstance leads to a decrease in decolorization efficiency. Conversely, at pH levels beyond the optimal range, ferrous ions become unstable and tend to

precipitate, forming ferrous and ferric hydroxides (as per Eq. (2)). These species impede the reaction between Fe^{2+} and H_2O_2, resulting in limited hydroxyl radical generation and a subsequent reduction in decolorization efficiency [46,47,50].

The synergistic impact of dye concentration and feed flow rate on decolorization efficiency is illustrated in Fig. 5. The findings, documented at a pH of 3.5, H_2O_2 concentration of 150 mg/l, ferrous ion concentration of 50 mg/L, and varying feed flow rates from 1 to 8 ml/min, demonstrate that, at a consistent flow rate, escalating dye concentration leads to a reduction in decolorization efficiency. This decline in efficiency with increasing dye concentration can be attributed to the insufficient availability of hydroxyl radicals for the degradation of all dye molecules.

In the Fenton process, the concentration of Fe^{2+} serves as a crucial catalyst that significantly impacts decolorization efficiency. Illustrated in Fig. 6, the decolorization efficiency trends across Fe^{2+} concentrations ranging from 0.5 to 4 mg/l depict an increase in efficiency with higher Fe^{2+} concentrations across all feed flow rates. This relationship can be elucidated by the direct proportionality between the production of hydroxyl radicals in the Fenton process and Fe^{2+} concentrations. As Fe^{2+} concentrations rise, there is a corresponding enhancement in decolorization efficiency.

Furthermore, the analysis of feed flow rate influences on decolorization efficiency across various operational conditions, as outlined in Figs. 3–6, reveals a decrease in decolorization efficiency with escalating feed flow rates. This decline can be attributed to the reduced contact time within the reactor resulting from increased feed flow rates.

4.4. Optimization

In this work, MATLAB (R2020b) optimization toolbox was employed by using of the function “GA”. The optimal problem at constant inlet Dye concentration could be expressed in the following equation (12):

$$f(x_i) = \max(\text{DecolorizationEfficiency}\%) \tag{12}$$

Where: x_i = pH, Inlet Flow rate (ml/min), Fe^{2+} and H_2O_2 Concentration (mg/l).

In tackling the optimization conundrum at hand, the decision variables, representing the pivotal operating parameters, were meticulously selected based on the stipulated boundaries outlined by Rahimi et al. [22], as delineated in Table 1. Employing a potent ANN model integrated with genetic algorithm techniques, the research sought to pinpoint the optimal operational parameters conducive to the maximization of the decolorization efficiency within the Fenton process framework [39,51–54]. The outcomes unveiled in Table 3 encapsulate the optimal operating parameters at distinct dye concentrations, as ascertained through the adept utilization of the developed ANN model in conjunction with the genetic algorithm optimization approach. Notably, the findings in Table 3 unequivocally underscore that peak decolorization efficiency at each dye concentration within the designated range of operating parameters (as detailed in Table 1) was concomitantly achieved at the minimal feed flow rate (maximum contact time), while simultaneously leveraging maximum levels of H_2O_2 and Fe^{2+} concentrations to amplify OH radical generation [25,26,55,56]. Moreover, maintaining the pH within the confines of 2.6–2.8 further augmented the efficacy of the Fenton process optimization endeavor.

The escalating dosages of H_2O_2 and Fe^{2+} coupled with the decreased feed flow rate and their favorable impact on enhancing decolorization efficiency have been elucidated earlier. Furthermore, the findings underscore a notable trend—amid identical operational settings, elevating dye concentrations yield optimum efficiency levels at lower pH values. This phenomenon can be attributed to the heightened effectiveness of hydroxyl radicals formation in acidic environment. Consequently, with a rise in dye concentration within the same operational context, it becomes imperative to foster an environment conducive to heightened hydroxyl radical production, consequently necessitating a reduction in the solution’s pH [22,28,57–59].

Delving into the optimal pH range as delineated in Table 3 warrants elucidation. Notably, existing literature, including references [21,30,59–61], advocates for a pH approximation of 3 as an optimal for the Fenton process. Consequently, the optimal pH range presented in this study harmonizes aptly with the values expressed in prior research endeavors, underscoring a good alignment with established scientific literature [62–65].

5. Conclusion

This article presents a comprehensive modeling approach employing artificial neural networks to facilitate the decolorization of the DR16 azo dye utilizing the Fenton process within a microchannel reactor setting. The pinnacle of this endeavor was the development of an optimal ANN model tailored for estimating the effluent dye concentration. This develped model comprises a three layers encompassing neurons distributed as 5, 5, and 1, respectively. Within this model’s construct, the neural network’s input variables contain pivotal parameters including the inlet flow rate, pH level, as well as the concentrations of the dye, Fe^{2+}, and H_2O_2. On the output, the network’s encapsulates the effluent dye concentration.

The comparative analysis between the experimental data and the outcomes generated by the proficiently developed ANN model unequivocally established the model’s adept predictive capabilities. The probing investigation into the operational parameters’ influence on the system’s performance, facilitated by the adept ANN model, unraveled key insights. Notably, the findings underscore the pivotal roles played by the pH level, feed flow rate, and concentrations of Fe^{2+}, H_2O_2, and the dye in steering the decolorization of DR16. Evidently, escalating concentrations of Fe^{2+} and H_2O_2 can influence in augmenting dye decolorization. Conversely, the diminish in dye concentration and feed flow rate induce adverse impact on decolorization efficiency. These findings underscore interplay between the operational variables and the decolorization efficacy within the experimental framework, shedding light on the

Table 3
The optimal operating conditions for maximization of decolorization efficiency of the Fenton process by using of microchannel reactor at 25 °C and different dye concentrations.

Case	Flow rate (ml/min)	$[H_2O_2]$ (mg/l)	$[Fe^{2+}]$ (mg/l)	pH	Max. Decolorization efficiency %
[DR16] = 10 mg/l	1.0	500.0	4.0	2.80	72.82
[DR16] = 20 mg/l	1.0	500.0	4.0	2.75	85.94
[DR16] = 30 mg/l	1.0	500.0	4.0	2.63	87.72
[DR16] = 40 mg/l	1.0	500.0	4.0	2.6	89.78

strategic optimization imperatives for system performance enhancement.

The synergistic integration of the developed ANN model with a genetic algorithm was leveraged to derive optimal operational parameters aimed at maximizing decolorization efficiency across varying dye concentrations. The outcomes unveiled that the peak decolorization efficiencies at 10, 20, 30, and 40 mg/l dye concentrations stood at 72.82 %, 85.94 %, 87.72 %, and 89.78 %, respectively. The meticulous calibration rendered the following optimal parameters: a feed flow rate of 1 ml/min, H_2O_2 concentration set at 500 mg/l, Fe^{2+} concentration at 4 mg/l, and a pH range spanning from 2.6 to 2.8.

CRediT authorship contribution statement

Jafar Sadeghzadeh Ahari: Writing – original draft, Software, Resources, Formal analysis, Data curation, Conceptualization. **Masoud Sadeghi:** Writing – original draft, Software, Methodology, Conceptualization. **Mahdi Koolivand Salooki:** Writing – review & editing, Methodology, Investigation, Data curation, Conceptualization. **Morteza Esfandyari:** Writing – review & editing, Supervision, Project administration, Data curation, Conceptualization. **Masoud Rahimi:** Writing – review & editing, Methodology, Investigation. **Sanaz Anahid:** Writing – original draft, Software, Resources, Methodology, Formal analysis, Conceptualization.

Declaration of competing interest

The authors declare that they have no known competing financial interests or personal relationships that could have appeared to influence the work reported in this paper.

References

[1] A. Dargahi, et al., Electrochemical degradation of 2, 4-Dinitrotoluene (DNT) from aqueous solutions using three-dimensional electrocatalytic reactor (3DER): degradation pathway, evaluation of toxicity and optimization using RSM-CCD, Arab. J. Chem. 15 (3) (2022) 103648.
[2] G.D. Değermenci, Decolorization of reactive azo dye by fenton and photo-fenton processes in aqueous solution: the influence of operating conditions, kinetics study, and performance comparison, Bull. Chem. Soc. Ethiop. 37 (1) (2023) 197–210.
[3] J. Modak, et al., Continuous decolorization of dye solution by homogeneous Fenton process in a rotating packed bed reactor, Int. J. Environ. Sci. Technol. 17 (2020) 1691–1702.
[4] D.R. Cruz, et al., Magnetic nanostructured material as heterogeneous catalyst for degradation of AB210 dye in tannery wastewater by electro-Fenton process, Chemosphere 280 (2021) 130675.
[5] A. Dargahi, et al., Enhanced electrocatalytic degradation of 2, 4-Dinitrophenol (2, 4-DNP) in three-dimensional sono-electrochemical (3D/SEC) process equipped with Fe/SBA-15 nanocomposite particle electrodes: degradation pathway and application for real wastewater, Arab. J. Chem. 15 (5) (2022) 103801.
[6] A. Dargahi, et al., Electro-peroxymonosulfate processes for the removal of humic acid from aqueous media, Biomass Conversion and Biorefinery (2022) 1–15.
[7] N. Chi, et al., Efficient removal of RR2 dye by electro-Ce (III) process with its elegant arts and attractive charm in performance, energy consumption and mechanism, Environ. Res. 216 (2023) 114590.
[8] A. Dargahi, et al., Highly effective degradation of 2, 4-Dichlorophenoxyacetic acid herbicide in a three-dimensional sono-electro-Fenton (3D/SEF) system using powder activated carbon (PAC)/Fe3O4 as magnetic particle electrode, J. Environ. Chem. Eng. 9 (5) (2021) 105889.
[9] A. Dargahi, et al., Applications of advanced oxidation processes (electro-Fenton and sono-electro-Fenton) for degradation of diazinon insecticide from aqueous solutions: optimization and modeling using RSM-CCD, influencing factors, evaluation of toxicity, and degradation pathway, Biomass Conversion and Biorefinery (2021) 1–18.
[10] A. Dargahi, et al., Evaluating efficiency of H2O2 on removal of organic matter from drinking water, Desalination Water Treat. 54 (6) (2015) 1589–1593.
[11] N. Daud, B. Hameed, Decolorization of Acid Red 1 by Fenton-like process using rice husk ash-based catalyst, J. Hazard Mater. 176 (1–3) (2010) 938–944.
[12] M.E. Farshchi, H. Aghdasinia, A. Khataee, Modeling of heterogeneous Fenton process for dye degradation in a fluidized-bed reactor: kinetics and mass transfer, J. Clean. Prod. 182 (2018) 644–653.
[13] M. Ghanbari, et al., Biodegradation of acid orange 7 dye using consortium of novel bacterial strains isolated from Persian Gulf water and soil contaminated with petroleum compounds, Biomass Conversion and Biorefinery 13 (15) (2023) 13695–13706.
[14] E. GilPavas, S. Correa-Sanchez, D.A. Acosta, Using scrap zero valent iron to replace dissolved iron in the Fenton process for textile wastewater treatment: optimization and assessment of toxicity and biodegradability, Environ. Pollut. 252 (2019) 1709–1718.
[15] E. GilPavas, I. Dobrosz-Gómez, M.Á. Gómez-García, Optimization of solar-driven photo-electro-Fenton process for the treatment of textile industrial wastewater, J. Water Proc. Eng. 24 (2018) 49–55.
[16] A.-R.A. Giwa, et al., Kinetic and thermodynamic studies of fenton oxidative decolorization of methylene blue, Heliyon 6 (8) (2020) e04454.
[17] B. Gowtham, S. Pauline, Performance Evaluation Studies of Fenton Oxidation on Different Dyes and its Optimization of Experimental Parameters, 2020.
[18] A. Hafizi, et al., Comparison of RSM and ANN for the investigation of linear alkylbenzene synthesis over H14 [NaP5W30O110]/SiO2 catalyst, J. Ind. Eng. Chem. 19 (6) (2013) 1981–1989.
[19] K. Hasani, et al., Enhancing the efficiency of electrochemical, Fenton, and electro-Fenton processes using SS316 and SS316/β-PbO 2 anodes to remove oxytetracycline antibiotic from aquatic environments, Biomass Conversion and Biorefinery (2021) 1–18.
[20] K. Hasani, et al., Evaluation of cefixime toxicity treated with sono-electro-fenton process by bioassay using microorganisms, Avicenna Journal of Environmental Health Engineering 8 (1) (2021) 22–27.
[21] V. Nourani, M.T. Alami, F.D. Vousoughi, Self-organizing map clustering technique for ANN-based spatiotemporal modeling of groundwater quality parameters, J. Hydroinf. 18 (2) (2016) 288–309.

[22] M. Rahimi, et al., Using Y-shaped microreactor for continuous decolorization of an Azo dye, Desalination Water Treat. 52 (28–30) (2014) 5513–5519.
[23] M. Quaglio, et al., An artificial neural network approach to recognise kinetic models from experimental data, Comput. Chem. Eng. 135 (2020) 106759.
[24] A. Adachi, et al., Decolorization and degradation of methyl orange azo dye in aqueous solution by the electro fenton process: application of optimization, Catalysts 12 (6) (2022) 665.
[25] M.R. Samarghandi, et al., Degradation of azo dye Acid Red 14 (AR14) from aqueous solution using H2O2/nZVI and S2O82–/nZVI processes in the presence of UV irradiation, Water Environ. Res. 92 (8) (2020) 1173–1183.
[26] A. Seid-Mohammadi, et al., Photocatalytic degradation of metronidazole (MnZ) antibiotic in aqueous media using copper oxide nanoparticles activated by H2O2/UV process: biodegradability and kinetic studies, Desalination Water Treat. 193 (2020) 369–380.
[27] S. Beldjoudi, et al., Experimental and theoretical investigation of a homogeneous Fenton process for the degradation of an azo dye in batch reactor, React. Kinet. Mech. Catal. 133 (1) (2021) 139–155.
[28] T. Mohapatra, et al., Hybrid fenton oxidation processes with packed bed or fluidized bed reactor for the treatment of organic pollutants in wastewater: a review, Environ. Eng. Sci. 38 (6) (2021) 443–457.
[29] K. Hasani, et al., The efficacy of sono-electro-Fenton process for removal of Cefixime antibiotic from aqueous solutions by response surface methodology (RSM) and evaluation of toxicity of effluent by microorganisms, Arab. J. Chem. 13 (7) (2020) 6122–6139.
[30] M.N. Patel, M. Shah, Feasibility study of Fenton method for the treatment of dyeing and printing mill wastewater, Int. J. Sci. Eng. Technol. 2 (5) (2013) 411–416.
[31] C.-C. Su, et al., Effect of operating parameters on the decolorization and oxidation of textile wastewater by the fluidized-bed Fenton process, Separ. Purif. Technol. 83 (2011) 100–105.
[32] M.K. Salooki, et al., Design of neural network for manipulating gas refinery sweetening regenerator column outputs, Separ. Purif. Technol. 82 (2011) 1–9.
[33] H. Salehi, et al., Designing a neural network for closed thermosyphon with nanofluid using a genetic algorithm, Braz. J. Chem. Eng. 28 (2011) 157–168.
[34] M. Shokouhi, et al., Thermodynamical and artificial intelligence approaches of H2S solubility in N-methylpyrrolidone, Chem. Phys. Lett. 707 (2018) 22–30.
[35] G.E. Box, D.A. Pierce, Distribution of residual autocorrelations in autoregressive-integrated moving average time series models, J. Am. Stat. Assoc. 65 (332) (1970) 1509–1526.
[36] N. Bravo-Yumi, et al., Studying the influence of different parameters on the electrochemical oxidation of tannery dyes using a Ti/IrO2-SnO2-Sb2O5 anode, Chemical Engineering and Processing-Process Intensification 181 (2022) 109173.
[37] M.K. Salooki, et al., Experimental and modelling investigation of H2S solubility in N-methylimidazole and gamma-butyrolactone, J. Chem. Therm. 135 (2019) 133–142.
[38] M. Takassi, et al., Neuro-fuzzy prediction of Fe-V2O5-promoted γ-alumina catalyst behavior in the reverse water–gas–shift reaction, Energy Technol. 1 (2-3) (2013) 144–150.
[39] M.A. Takassi, et al., Neuro-Fuzzy prediction of alumina-supported cobalt vanadate catalyst behavior in the Fischer-Tropsch process, Eur. J. Chem. 4 (2) (2013) 110–116.
[40] N. Saghatoleslami, M. Salooki, N. Mohamadi, Auto-design of neural network–based GAs for manipulating the khangiran gas refinery sweetening absorption column outputs, Petrol. Sci. Technol. 29 (14) (2011) 1437–1448.
[41] J. Anmala, et al., GIS and artificial neural network–based water quality model for a stream network in the Upper Green River Basin, Kentucky, USA, J. Environ. Eng. 141 (5) (2015) 04014082.
[42] S. Ascher, et al., A comprehensive artificial neural network model for gasification process prediction, Appl. Energy 320 (2022) 119289.
[43] F.M. Cavalcanti, et al., A catalyst selection method for hydrogen production through Water-Gas Shift Reaction using artificial neural networks, J. Environ. Manag. 237 (2019) 585–594.
[44] Y. Chen, et al., A review of the artificial neural network models for water quality prediction, Appl. Sci. 10 (17) (2020) 5776.
[45] V.T. Le, et al., Artificial neural networks for predicting hydrogen production in catalytic dry reforming: a systematic review, Energies 14 (10) (2021) 2894.
[46] Z. Yao, C. Romero, J. Baltrusaitis, Combustion optimization of a coal-fired power plant boiler using artificial intelligence neural networks, Fuel 344 (2023) 128145.
[47] A. Zare, V. Bayat, A. Daneshkare, Forecasting nitrate concentration in groundwater using artificial neural network and linear regression models, Int. Agrophys. 25 (2) (2011).
[48] J.H. Holland, Genetic algorithms and adaptation. Adaptive Control of Ill-Defined Systems, 1984, pp. 317–333.
[49] D. Kumar, S.K. Gupta, Electrochemical oxidation of direct blue 86 dye using MMO coated Ti anode: modelling, kinetics and degradation pathway, Chemical Engineering and Processing-Process Intensification 181 (2022) 109127.
[50] L. Zhang, Z. Zou, W. Shan, Development of a method for comprehensive water quality forecasting and its application in Miyun reservoir of Beijing, China, J. Environ. Sci. 56 (2017) 240–246.
[51] A. Seidmohammadi, et al., A comparative study for the removal of methylene blue dye from aqueous solution by novel activated carbon based adsorbents, Progress in Color, Colorants and Coatings 12 (3) (2019) 133–144.
[52] A. Seidmohammadi, et al., Improved degradation of metronidazole in a heterogeneous photo-Fenton oxidation system with PAC/Fe 3 O 4 magnetic catalyst: biodegradability, catalyst specifications, process optimization, and degradation pathway, Biomass Conversion and Biorefinery (2021) 1–17.
[53] R. Shokoohi, et al., Investigation of the efficiency of heterogeneous Fenton-like process using modified magnetic nanoparticles with sodium alginate in removing Bisphenol A from aquatic environments: kinetic studies, Desalination Water Treat. 101 (2018) 185–192.
[54] X.-R. Xu, et al., Chemical oxidative degradation of methyl tert-butyl ether in aqueous solution by Fenton's reagent, Chemosphere 55 (1) (2004) 73–79.
[55] M.R. Samarghandi, et al., Electrochemical degradation of methylene blue dye using a graphite doped PbO2 anode: optimization of operational parameters, degradation pathway and improving the biodegradability of textile wastewater, Arab. J. Chem. 13 (8) (2020) 6847–6864.
[56] A. Seid-Mohammadi, et al., The removal of cephalexin antibiotic in aqueous solutions by ultrasonic waves/hydrogen peroxide/nickel oxide nanoparticles (US/H2O2/NiO) hybrid process, Separ. Sci. Technol. 55 (8) (2020) 1558–1568.
[57] M. Heidari, et al., Degradation of diazinon from aqueous solutions by electro-Fenton process: effect of operating parameters, intermediate identification, degradation pathway, and optimization using response surface methodology (RSM), Separ. Sci. Technol. 56 (13) (2021) 2287–2299.
[58] A. Mohammadifard, et al., Synthesis of magnetic Fe3O4/activated carbon prepared from banana peel (BPAC@ Fe3O4) and salvia seed (SSAC@ Fe3O4) and applications in the adsorption of Basic Blue 41 textile dye from aqueous solutions, Appl. Water Sci. 12 (5) (2022) 88.
[59] S.A. Mokhtari, et al., Removal of polycyclic aromatic hydrocarbons (PAHs) from contaminated sewage sludge using advanced oxidation process (hydrogen peroxide and sodium persulfate), Desalination Water Treat. 213 (2021) 311–318.
[60] A. Peyghami, et al., Evaluation of the efficiency of magnetized clinoptilolite zeolite with Fe3O4 nanoparticles on the removal of basic violet 16 (BV16) dye from aqueous solutions, J. Dispersion Sci. Technol. 44 (2) (2023) 278–287.
[61] P. Pourali, et al., Enhanced three-dimensional electrochemical process using magnetic recoverable of Fe3O4@ GAC towards furfural degradation and mineralization, Arab. J. Chem. 15 (8) (2022) 103980.
[62] A. Rahmani, et al., The integration of PbO2-based EAOPs with other advanced oxidation processes for improved treatment of water and wastewater, Curr. Opin. Electrochem. 37 (2023) 101204.
[63] A.R. Rahmani, et al., Enhanced degradation of Rhodamine B dye by Fenton/peracetic acid and photo-Fenton/peracetic acid processes, Int. J. Chem. React. Eng. 20 (12) (2022) 1251–1260.
[64] T. Rajaee, A. Boroumand, Forecasting of chlorophyll-a concentrations in South San Francisco Bay using five different models, Appl. Ocean Res. 53 (2015) 208–217.
[65] F. Rivas, et al., Simazine Fenton's oxidation in a continuous reactor, Appl. Catal. B Environ. 48 (4) (2004) 249–258.